

# Trajectory design of ERO alternative return towards a lunar Distant Retrograde Orbit

Lorenzo Bucci<sup>(1)</sup>, José Manuel Sánchez Pérez<sup>(2)</sup>, Laurent Beauregard<sup>(3)</sup>, Alessandro Masat<sup>(4)</sup>, Amedeo Rocchi<sup>(5)</sup>

<sup>(1)</sup>*Deimos Space S.L.U. at ESA-ESOC  
Darmstadt, Germany  
Lorenzo.Bucci@ext.esa.int*

<sup>(2)</sup>*European Space Agency, ESA-ESOC  
Darmstadt, Germany  
Jose.Manuel.Sanchez.Perez@esa.int*

<sup>(3)</sup>*Telespazio Germany GmbH at ESA-ESOC  
Darmstadt, Germany  
Laurent.Beauregard@ext.esa.int*

<sup>(4)</sup>*IMS Space Consultancy at ESA-ESOC  
Darmstadt, Germany  
Alessandro.Masat@ext.esa.int*

<sup>(5)</sup>*GMV at ESA-ESOC  
Darmstadt, Germany  
Amedeo.Rocchi@ext.esa.int*

**Abstract** – Due to programmatic and technology development constraints alternative architectures are under consideration for the international NASA-ESA Mars Sample Return (MSR) campaign. One of such alternatives envisages the Earth Return Orbiter (ERO) delivering the Mars samples to an intermediate parking orbit in the Earth-Moon system, namely a lunar Distant Retrograde Orbit (DRO). A future mission will then retrieve the samples and bring them to Earth. This paper analyses the alternative return scenario and describes in detail the trajectory design process.

## I. INTRODUCTION

ERO, ESA's main contribution to the NASA-ESA MSR campaign [1], is a hybrid Electric Propulsion (EP) – Chemical Propulsion (CP) spacecraft with a large 41-kW-class 144 m<sup>2</sup> solar array to operate solar EP system at Mars. The main goal of ERO is to capture the Mars samples (once injected in Low Mars Orbit) and return them to Earth. The baseline mission scenario for ERO mission considers a direct return to Earth releasing an Earth Entry Vehicle (EEV) from the hyperbolic approach, and performing an Earth Avoidance Manoeuvre to guarantee heliocentric disposal of the spacecraft in compliance with backward planetary protection requirements [2].

In the context of feasibility assessment of alternative architectures, the ERO's ESA mission analysis team studied delivering the samples to a lunar DRO. Using the on-board EP system, the ERO spacecraft would depart from low Mars orbit and reach the Earth with a reduced infinite velocity (<1.5 km/s). A distant Earth flyby would be followed by a lunar gravity assist (LGA)

that reduces the geocentric energy enough to reach the Weak Stability Boundary (WSB), where the Sun's gravity is exploited to raise the perigee until the lunar altitude. A second LGA would be performed prior to finally injecting the spacecraft into a lunar DRO. A similar endgame trajectory was identified for NASA's Asteroid Redirect Robotic Mission [3].

The DRO is chosen for its good reachability from Earth as well as its stability properties; the paper shows how such orbit can be designed with an initial guess in the Circular Restricted Three-Body Problem, and then refined with numerical optimization to guarantee its stability for 100 years, complying with strict backwards planetary protection requirements. Additionally, the recovered samples shall remain in orbit until a retrieval mission is performed, hence the DRO stability ensures no station-keeping is required and ERO can safely end its mission.

The proposed endgame trajectory in the Earth-Moon-Sun system takes roughly 3 months from Earth fly-by to DRO injection. Avoiding long eclipses is also one of the goals of the trajectory design; DRO injection would be followed by an eclipse-free period of at least 100 days.

Additionally, the paper mentions alternative options, changing the sequence of flybys prior to reaching the DRO, or adding a 1:1 resonant arc to exploit v-infinity leveraging and further reduce the overall  $\Delta v$  budget.

## II. DISTANT RETROGRADE ORBITS (DRO)

### A. Orbit family

The DRO family derives from low, retrograde, equatorial lunar orbits. The retrograde motion allows to exploit the Earth perturbation to achieve long-term stability. As the amplitude of these orbits grows higher, the gravity of the Earth becomes more and more relevant, affecting the shape of the orbit and leading to an elongation along the  $y$ -axis of the Earth-Moon rotating frame. Fig. II-1 depicts some DROs in the range of interest for this study, integrated using the Circular Restricted Three-Body Problem (CR3BP) dynamical model.

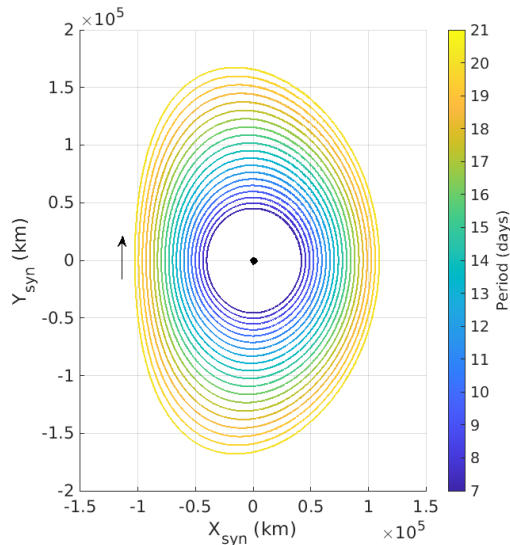


Fig. II-1: DROs in the Earth-Moon rotating frame.

Within this document, the concept of mean anomaly is used to define the position along the DRO. This value, not strictly valid for non-Keplerian orbits, can be used to have an intuitive figure to quantify the motion along the orbit. Assuming the DROs “start” at the  $xy$ -plane crossing between the Earth and the Moon, it is possible to define the mean anomaly as

$$M(t) = \frac{2\pi t}{T} \quad (1)$$

where  $t$  is the time spent from the reference starting point and  $T$  the period in the CR3BP.

### B. Stability in the full-ephemeris model

In the ephemeris model, the DROs states need to be modified with respect to the CR3BP ones, to ensure long term stability. In this context, stability means a DRO is robust to injection errors and perturbations. To perform this analysis, a stability criterion was defined, such that a trajectory is valid for  $N$  years if it does not intersect the spheres of 20,000 km and 200,000 km around the Moon for  $N$  years.

Scanning the  $x$ - position and the  $y$ - velocity in the Earth-Moon rotating frame, several regions of stability are identified, as depicted in Fig. II-2:

1. “Classical” Keplerian Moon orbits (potentially unstable due to unmodelled Moon harmonics at low periapsis)
2. “Normal” DROs, extremely stable
3. Small island of stability  $\sim 52,000$  km
4. Large island of stability  $\sim 65,000$  km
5. Chaotic region, small stability region mixed with unstable regions  $\sim 70,000$  to  $80,000$  km
6. Quasi-stable high amplitude DRO  $\sim 100,000$  km

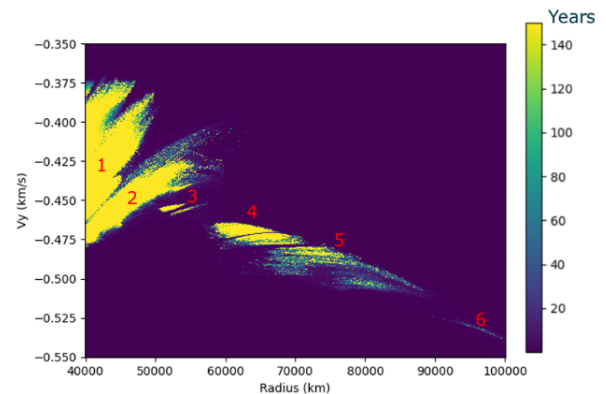


Fig. II-2: DRO stability regions.

The wide region 4 is found to be a good candidate for the target DRO. A test for robustness has been performed by running a Monte-Carlo with random initial perturbations in position and velocity, simulating injection errors and unmodeled perturbations. The candidate DRO (62,000 km) is robust to perturbations up to 3 m/s in velocity and 800 km in position.

## III. HELIOCENTRIC INBOUND TRANSFER

### A. Overview

ERO will make use of its on-board EP to leave Low Mars Orbit spiralling up until Mars Sphere Of Influence (SOI) and then lowering the heliocentric orbit up until reaching the Earth. While the spiral-up phase remains unaffected by the decision to deliver the samples to a lunar DRO, and is therefore not regarded in this analysis, the heliocentric Inbound Transfer Phase (ITP) requires significant adjustment.

A pre-requisite to reaching a lunar DRO is to get captured in the Earth-Moon system. In order to achieve this by means of a single LGA, it is necessary to arrive at the Earth with an infinite velocity below 1.5 km/s; well below the 3.5 km/s of the baseline mission for samples delivery via an EEV. In addition, the arrival at the Earth would need to occur when the Earth-Moon-Sun geometry is favourable for the endgame.

A sensitivity analysis of the ITP to the Earth arrival date and infinite velocity is depicted in Fig. III-1. Latest departure from Mars SOI is set to 2035-01-07 for compatibility with ERO's operations in Mars orbit and the spiral-up phase. The plot is centred around MJD2000 (=days since 2000-01-01) of 13170, which refers to 2036-01-22; the range is about  $\pm 40$  days thus capturing over 2 orbital periods of the Moon. Roughly 4200 m/s and 4700 m/s EP  $\Delta v$  are required to achieve an Earth infinite velocity of 1.5 km/s and 1.0 km/s, respectively. Such ITP  $\Delta v$  is much larger than the roughly 2500 m/s for the direct Earth return in October 2033 of the current baseline design and would only be achievable by decreasing ERO's return dry mass.

The red curves indicate transfers that arrive at the Moon for LGA1 with a fixed infinite velocity of roughly 1.3 km/s, tuned for a preliminary solution of the endgame trajectory (blue circle). Sensitivity of  $\Delta v$  to the arrival date is much stronger, and in some cases, it is not feasible to achieve the desired infinite velocity. Remarkably, Earth-Moon-Sun geometries favourable for the endgame do not coincide with the minimum of the ITP  $\Delta v$ .

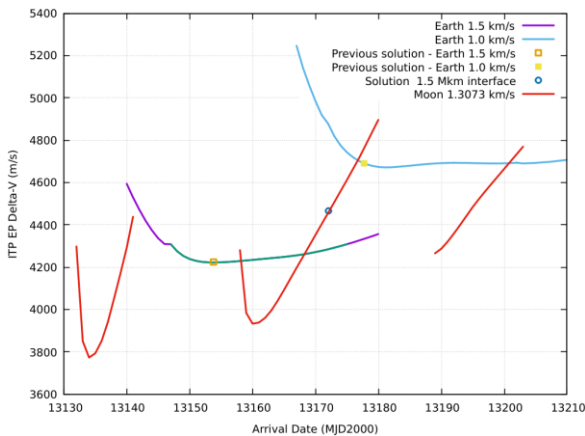


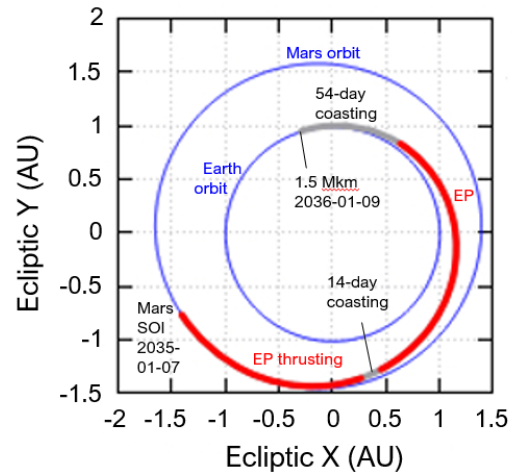
Fig. III-1: Sensitivity of ITP  $\Delta v$  to arrival date.

### B. Matching with the endgame

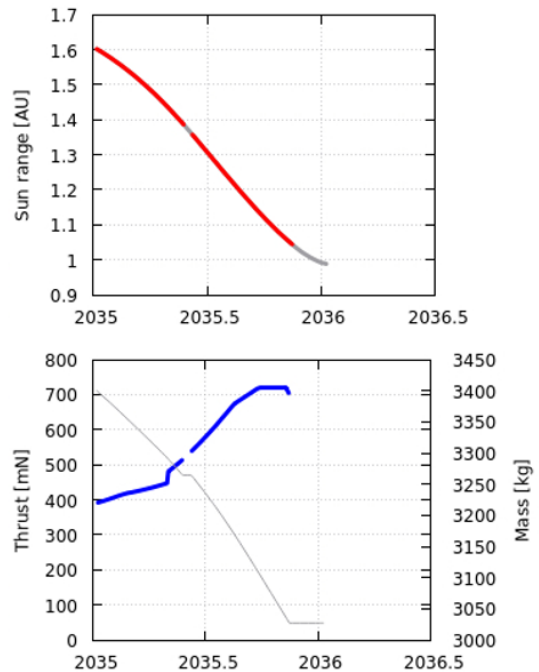
During the trajectory design, the heliocentric ITP trajectory and endgame trajectory are calculated separately by independent tools. An interface point 1.5 million km from Earth is defined between these two trajectories. To ensure continuity of the overall trajectory ERO's state vector with respect to Earth at the interface point is targeted forwards by the inbound transfer and backwards from LGA1 by the endgame trajectory. This state vector has been obtained via an iterative process that converged nicely in a few steps.

The optimised heliocentric ITP trajectory, details depicted by Fig. III-2, requires 4542 m/s when calculated with the high-fidelity force model by our GODOT tool [5]. Notice that the EP thrust magnitude

follows the complex dependency with the distance to the Sun dictated by the ERO platform.



a) Ecliptic trajectory projection.



b) Distance to the Sun, thrust magnitude and mass.

Fig. III-2: Heliocentric ITP trajectory.

Arrival date at the interface point is 2036-01-09, for a time of flight from Mars SOI of 367 days, and relative velocity to Earth is 1.172 km/s. The ITP trajectory is fully saturated with EP thrusting except for an intermediate 14-day coasting arc and a final 66-day coasting arc. It takes 12 days from the interface point to the perigee of the Earth flyby. The final coasting arc provides time margin for compensating missed thrust events along the heliocentric trajectory. It is however drastically reduced from about 120 days present in the current baseline for delivery with EEV.

#### IV. ENDGAME TRAJECTORY DESIGN

The endgame trajectory aimed at delivering ERO to the target DRO consists of the following main steps:

- Earth and Lunar gravity assists, this may involve first an Earth flyby and then a Moon flyby or the inverse order; the objective is to get weakly captured in the Earth-Moon system.
- Weak Stability Boundary (WSB) transit to exploit the Sun's gravity effect.
- One (or more) Lunar Gravity Assist (LGA)
- Insertion into the target DRO using the on-board propulsion.

The transfer is designed using the Sun, Earth and Moon point mass gravities and impulsive manoeuvres, then refined in a more complete dynamical model taking into account the gravity potential expansions of the Moon and the Earth and continuous-thrust manoeuvres.

The analysis starts from an interface point, set at 1.5 million km from Earth, whose state and epoch are known and derived from the interplanetary transfer.

##### A. Targeting the first lunar flyby

The most promising solution, given the Earth-Moon system configuration at the arrival date, is to have a high-altitude EGA followed by a lunar gravity assist (LGA1). This sequence is called Earth-Luna-Gravity Assist (ELGA), and the schematic geometry is depicted in Fig. IV-1.

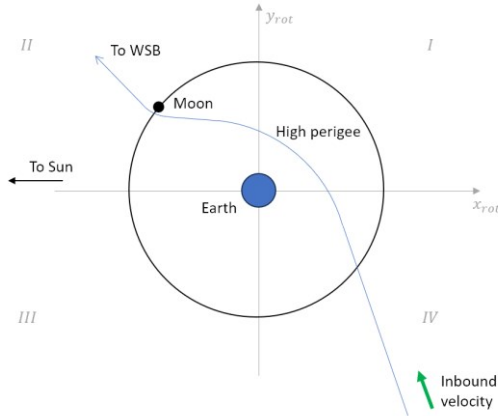


Fig. IV-1: Geometry of ELGA in the Sun-Earth rotating frame.

Note that this geometry is not the only option available; in theory, a total of four cases could be analysed, according to:

- The sequence of Earth-Moon flybys (Earth first or Moon first – i.e. ELGA or LEGA)
- The WSB transfer geometry (II or IV quadrant)

The LGA1 targeting requires finding the initial conditions to connect the incoming hyperbola with the Moon, which should be located in the II quadrant, such

that a subsequent WSB transfer is possible. The following parameters are optimized:

- Starting date (+/- 14 days with respect to the nominal value).
- Position of the incoming  $V_\infty$  vector.

Additionally, the  $V_\infty$  vector is allowed to vary +/- 20 m/s on each cartesian component.

The initial guess for the LGA1 targeting can be found by imposing two conditions:

1. The outgoing asymptote after the EGA,  $\mathbf{v}_{out}$ , shall be coplanar with the Moon orbital plane, for the LGA1 to be physically possible.
2. The angle between the Sun direction and the outgoing asymptote,  $\mathbf{v}_{out}$ , shall be such that the LGA1 is encountered towards the II quadrant.

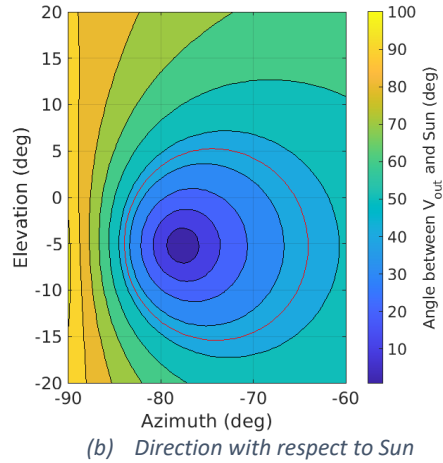
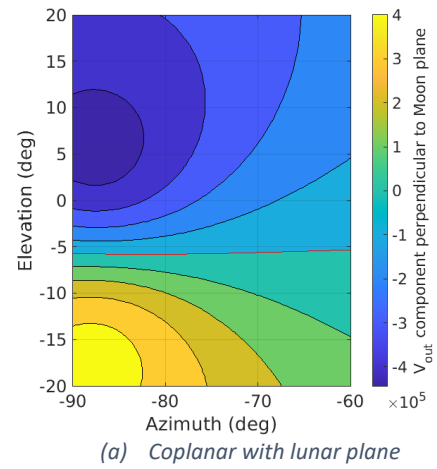


Fig. IV-2: Azimuth-elevation maps of the outgoing asymptote after the EGA for LGA1 targeting.

Fig. IV-2 depicts visual maps to identify the two aforementioned conditions. The matching between  $\mathbf{v}_{out}$  and the lunar orbital plane is identified as the locus of points which nulls the dot product between  $\mathbf{v}_{out}$  and the angular momentum of the Moon (Fig. IV-2a). The WSB “direction” is identified by the angle between  $\mathbf{v}_{out}$  and

the Sun direction (Fig. IV-2b), looking for locus of points where this angle is 45 degrees (approximately pointing toward the II quadrant, as per Fig. IV-1). The intersection between the two curves provides the initial guess for the direction of  $\mathbf{v}_{out}$ .

### B. Weak Stability Boundary (WSB) phase

Once the location of the starting point is identified such that LGA1 is encountered, the second stage of the solution is to adjust the LGA1 parameters to reach the WSB. The approach consists in placing a point in the WSB region and propagating backwards, looking for a match with LGA1.

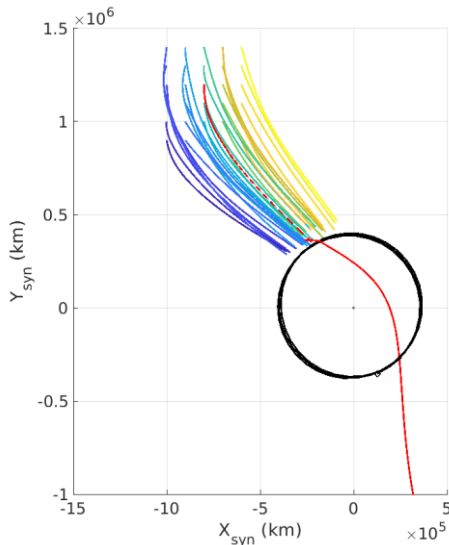


Fig. IV-3: Scan of the WSB region to patch with LGA1.

Fig. IV-3 depicts a scan, placing a point in the WSB region with null velocity in the Sun-Earth rotating frame. The x- and y-coordinates are varied in the intervals  $[-1e6, -6e5]$  km and  $[9e5, 1.4e6]$  km, respectively. The WSB points are propagated backwards in time, until they cross the Moon's orbit trace.

This method is purely geometric, so it does not take into account the actual motion of the Moon, nor a possible out-of-plane motion. These two quantities will be adjusted in the optimization step – this method aims at generating a sufficiently good initial guess.

### C. Targeting the second lunar flyby

After finding a good initial guess of the WSB phase, the second lunar flyby (LGA2) can be designed with a similar approach.

Taking the WSB state (with zero velocity in the Sun-Earth rotating frame), a  $\Delta v$  can be applied to target again the lunar orbit. In this case, it is expected that the second Moon encounter takes place in the III quadrant. Again, this solution is purely geometric, and an optimisation

process is then required to tune the Moon phasing to obtain a second flyby.

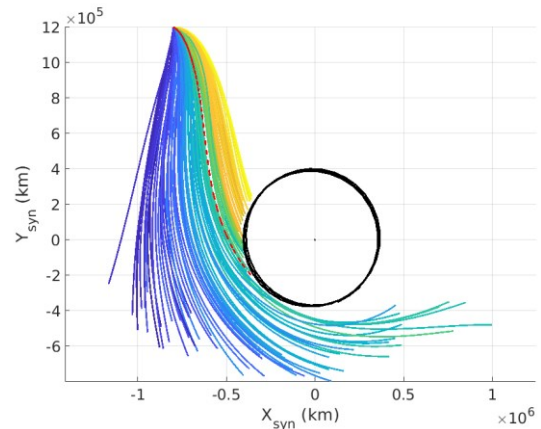


Fig. IV-4: Scan of the WSB region  $\Delta v$  to target LGA2.

Fig. IV-4 depicts the scan, varying the  $\Delta v$  applied to the WSB state to target LGA2. Note that the colormap has no physical meaning, but it's merely used to distinguish the different trajectories. The most promising solution was identified with  $\Delta v_x = 110$  m/s,  $\Delta v_y = -50$  m/s (dashed red line) and used as initial guess. Note that the  $\Delta v$  is expressed in the Sun-Earth rotating frame; this has the advantage of maintaining the same geometrical shape, independently of the epoch.

### D. Reaching the DRO

The final phase of the trajectory aims for capture into a DRO. This study initially targeted an  $80,000 \times 120,000$  km DRO with a 16-day period; the amplitude was changed at later stages to 62,000 km to improve long-term stability (see Section II.B).

The first analyses were devoted to finding a transfer to the DRO. The DRO is intrinsically stable in the CR3BP, so there is no stable manifold to exploit for a free injection. Nevertheless, low-energy transfers exist, requiring a  $\Delta v$  around 50 m/s.

A scan was performed applying a  $\Delta v$  of 50 m/s in the velocity direction at different locations along the DRO. Two dynamical structures can be identified, as depicted in Fig. IV-5:

- The interior transfers, in the mean anomaly range  $[90, 270]$  deg. They arrive from the Earth's side, perform a lunar flyby with the pericentre on the -y side, and after one loop they inject on the exterior side of the DRO.
- The exterior transfers, in the mean anomaly range  $[-90, 90]$  deg. They arrive from the exterior side, perform a lunar flyby with the pericentre on the +y side, and after one loop they inject on the Earth's side of the DRO.

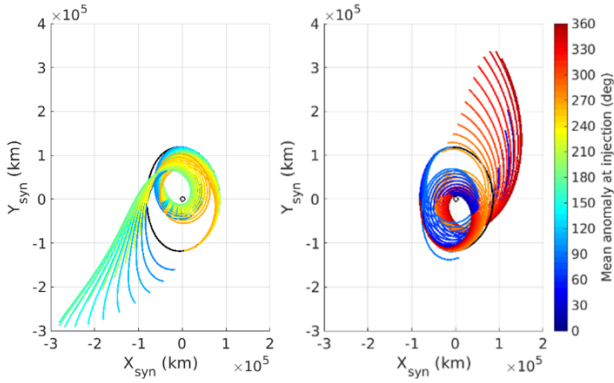


Fig. IV-5: Study of DRO injection and arrival in the Earth-Moon rotating frame.

Generally, the spacecraft is expected to arrive from the WSB to the exterior side of the Earth-Moon system. The initial guess will then be built with a 0 deg mean anomaly, an insertion  $\Delta v$  of 50 m/s, and the LGA2 pericentre on the +y-direction of the Earth-Moon rotating frame.

#### E. Patching the problem together

Once all the segments are solved, a single optimisation problem can be formulated to find an optimal solution of the full endgame. After transcription of the initial guess, the problem is solved with impulsive manoeuvres.

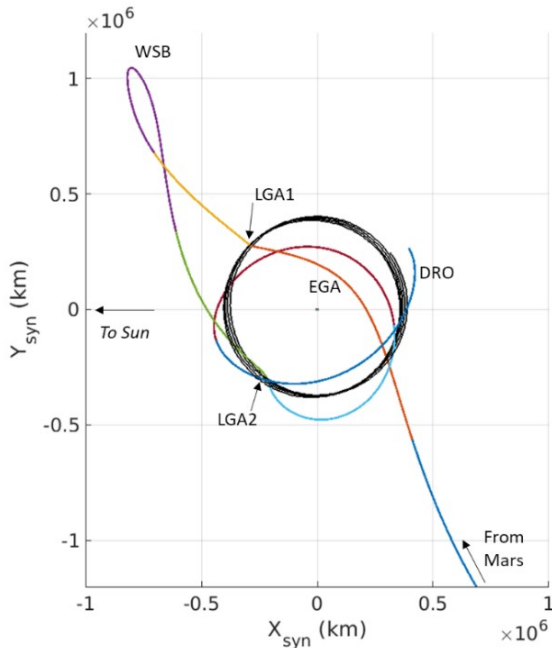


Fig. IV-6: Endgame solution, Sun-Earth rotating frame.

Fig. IV-6 and Fig. IV-7 depict the final trajectory. It is interesting to note that the final DRO injection shifts to the exterior side (at a mean anomaly of about 180 degrees), with respect to the initial guess in the interior side. This is due to the limitations of the CR3BP, which

anyway proves to provide a good initial guess to the final optimisation.

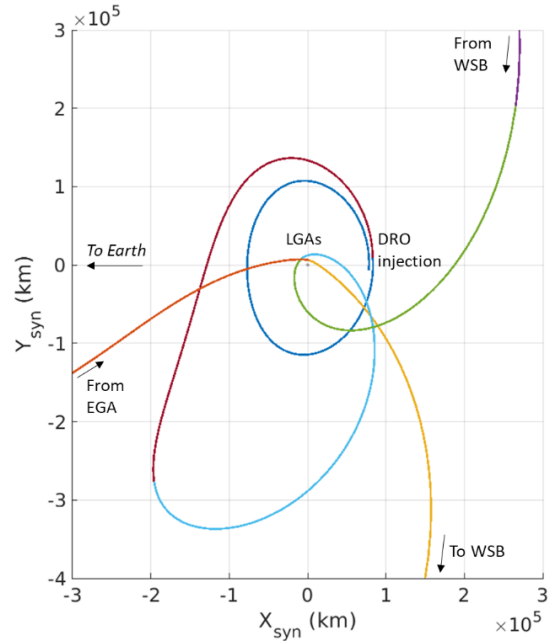


Fig. IV-7: Endgame solution, Earth-Moon rotating frame.

The total impulsive  $\Delta v$  is 67 m/s, including a 3 m/s manoeuvre after the WSB. After this step, the endgame solution is patched together with the interplanetary transfer, freeing the interface point and optimizing all the problem together (including finite-burn manoeuvres for the endgame phase). This final optimization results in an additional 30 m/s saving, and the full phase from LGA1 to DRO insertion is ballistic (except for TCMs).

## V. ADDITIONAL OPTIONS

### A. Alternative with EGA- $\Delta V$ and $V_\infty$ leveraging

A potential technique to reduce the EP  $\Delta v$  required for the Mars-Earth inbound leg was investigated. The concept of  $V_\infty$  leveraging is well known to reduce launch energy using a  $\Delta V$ -EGA, deep space manoeuvre (DSM) followed by Earth gravity assist [8]. The reverse sequence, namely EGA- $\Delta V$ , Earth gravity assist followed by a DSM, can be used to lower the Earth infinite velocity more efficiently than in the direct return to Earth. The arrival of the samples would be delayed by approximately 1 year, the duration of the Earth-DSM-Earth leg.

Return EGA- $\Delta V$  trajectories were calculated for minimum EP  $\Delta v$  to reach Earth with infinite velocity in range from 1.0 km/s to 1.5 km/s. Departure from Mars SOI occurs on December 2034, a few weeks earlier than for the direct return described in Section III. The optimal EGA takes place on 2025-12-10 at an infinite velocity

between 2.23 and 2.29 km/s and the DSM burn, optimally located around the 0.95 AU perihelion, requires 330 to 500 m/s. The overall ITP EP  $\Delta v$  saving ranges from 215 m/s to 540 m/s. The direction of the incoming infinite velocity vector at Earth is different from the one of direct return, hence the endgame trajectory would need a dedicated design, should this option be attractive to the ERO mission.

### B. LEGA strategies

The ELGA sequence presented throughout the paper was found to be optimal and satisfy the mission requirements. Nevertheless, additional solutions can be found for the transfer part, prior to injecting into the DRO.

An alternative solution of particular interest consists in having the LGA right after arrival from the interplanetary leg, followed by the EGA and the WSB phase.

This LEGA structure would enable arrival with a higher infinite velocity, but wasn't found of particular interest for the problem at hand. The optimal solution for the LEGA sequence is found about 20 days after the nominal interplanetary arrival, and this delay would lead to a high penalty in the interplanetary transfer phase. Conversely, the same solution computed one lunar month earlier (i.e. 9 months before the nominal arrival) is less favourable in terms of geometry and led to a higher overall  $\Delta v$ .

Additionally, another solution structure was found, adding a third lunar flyby before injecting into the DRO. This solution consists of a pi-transfer between LGA2 and LGA3, which allows to reach the DRO plane with lower  $\Delta v$  after the WSB arrival. Nevertheless, both the LEGA solutions where overall more expensive (including the navigation budget) than the current ELGA baseline and were discarded.

## VI. PLANETARY PROTECTION COMPLIANCE ANALYSIS

Being ERO permanently captured in the Earth-Moon system, the compliance of the DRO-returning trajectory with the Backward Planetary Protection requirements needs to be assessed. In particular, the contamination probability of either Earth or the Moon with Martian particles must be lower than  $10^{-6}$  for the 100 years following the beginning of the mission, with a 99% confidence level [6].

The analysis is performed by running Monte Carlo simulations at every manoeuvring point in the endgame trajectory, using CUDAjectory, an in-house GPU-based tool [7]. The uncertainty measures are the results of a

preliminary navigation covariance analysis, which are propagated forward in time assuming that the control of ERO is lost prior to the execution of each manoeuvre. Fig. VI-1 shows the evolution of the 100-year cumulative collision probability of ERO with Earth and the Moon, when no control action is implemented.

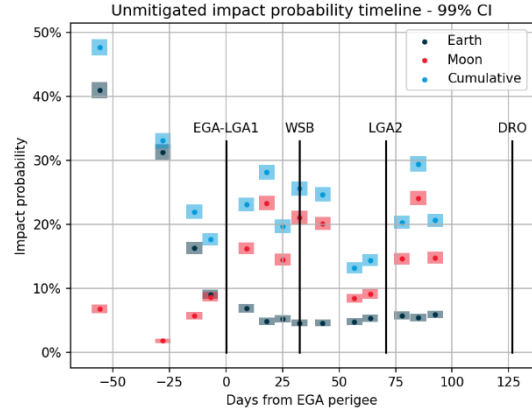


Fig. VI-1: Unmitigated collision probability timeline

At no point in the whole timeline the impact probability falls below planetary protection-compliant values, thus requiring the design of disposal strategies.

Until LGA2 occurs, 50 m/s impulsive  $\Delta v$  directions that deviate the endgame trajectory toward a heliocentric escape can be found, as shown in Fig. VI-2 for the 7-day LGA2 targeting manoeuvre point. Hence, provided that the execution of such impulsive manoeuvres is accurate enough, effective disposal solutions can be found for the most part of the endgame trajectory.

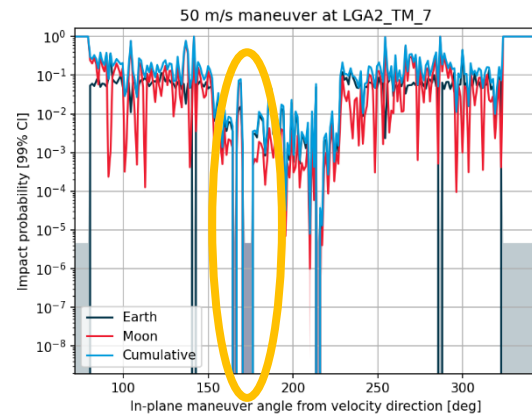


Fig. VI-2: 50 m/s impulsive disposal at the 7-day targeting manoeuvre (TM7) for LGA2

Nonetheless, after the occurrence of LGA2 ERO is permanently captured in the Earth-Moon system, making the budgeted 50 m/s  $\Delta v$  for disposal not enough to introduce stable heliocentric escape options. As the policies only demand the non-contamination of the Terrestrial and the Lunar environments with Martian particles, ERO can remain in the Earth-Moon system, as

long as its cumulative collision probability with either body remains below the given threshold [6]. Consequently, the safe option for ERO's disposal after LGA2 coincides with the remaining of the endgame timeline. In other words, ERO must be injected into a stable DRO belonging to the family presented in Section II.B, even in the case of spacecraft loss.

## VII. CONCLUSION

The paper presented a comprehensive feasibility assessment for the proposed alternative mission option, targeting a lunar DRO for the return of ERO. The study focused on the trajectory design, showing feasibility of the full return trajectory from Mars to DRO, and detailing the design methodology for the endgame (from Earth return to DRO insertion).

Additionally, the stability properties of the DRO where investigated, selecting a suitable candidate robust to perturbations and injection errors. Dedicated backwards planetary protection analysis has been performed highlighting the challenges associated with the endgame trajectory, and devising disposal strategies to meet the requirements at any point of the endgame timeline. Additional options for the return trajectory were preliminary explored, paving the way for future studies on further alternative scenarios.

In summary, no showstopper has been identified and consolidated results are provided for the consideration of the ERO mission.

## VIII. REFERENCES

- [1] T. Martin-Mur, J. M. Sánchez Pérez, R. Wilson, Z. Olikara, M. Jesick, R. Patel and D. Spencer, "The NASA/ESA Mars Sample Return Campaign," in *International Symposium on Space Flight Dynamics*, Darmstadt, 2024.
- [2] J. M. Sánchez Pérez, A. Rocchi, I. Acedo, M. Van den Broeck, O. Ramírez Torralba and S. Proietti, "ERO Consolidated Report on Mission Analysis", Darmstadt, 2023.
- [3] N. Strange, D. Landau, T. McElrath, G. Lantoine and T. Lam, "Overview of Mission Design for NASA Asteroid Redirect Robotic Mission Concept", IEPC-2013-321, in *33rd International Electric Propulsion Conference*, Washington, D.C., USA, 2013.
- [4] G. Turner, "Results of Long-Duration Simulation of Distant Retrograde Orbits", *Aerospace* 3.4 (2016): 37.
- [5] "GODOTPY documentation," [Online]. Available: <https://godot.io.esa.int/godotpy/>.
- [6] COSPAR - Committee on Space Research, "Cospar policy on planetary protection," *Space Research Today*, vol. 208, pp. 10–22, Aug. 2020. DOI: [10.1016/j.lssr.2023.02.001](https://doi.org/10.1016/j.lssr.2023.02.001)
- [7] M. Geda, R. Noomen, and F. Renk, "Massive Parallelization of Trajectory Propagations using GPUs," *Master's thesis, Delft University of Technology*, 2019. Available: [online](#)
- [8] J. Sims and J. Longuski, "Analysis of  $V_\infty$  leveraging for interplanetary missions," AIAA 1994-3769. *Astrodynamics Conference*. August 1994.